To appear in: The Astronomical Journal

A large spectroscopic survey for young low-mass members of the Upper Scorpius OB Association

Thomas Preibisch[1]
Max-Planck-Institut für Radioastronomie, Auf dem Hügel 69, D–53121 Bonn, Germany

Eike Guenther
Thüringer Landessternwarte Tautenburg, Sternwarte 5, D–07778 Tautenburg, Germany

Hans Zinnecker
Astrophysikalisches Institut Potsdam, An der Sternwarte 16, D–14482 Potsdam, Germany

ABSTRACT

We present the results of a large intermediate-resolution spectroscopic survey for pre-main sequence (PMS) stars in the Upper Scorpius OB association, the most nearby region of recent massive star formation. Utilizing the multi-object spectrograph 2dF at the Anglo-Australian-Telescope, we obtained spectra of 576 stars with magnitudes $R = [12.5 \ldots 16.5]$ in a 6 square-degree area in Upper Scorpius. Among these objects we were able to identify 98 new PMS stars, nearly all of them M-type stars, by their strong lithium absorption lines. We place the new PMS stars into the HR diagram and find that their ages agree well with the mean age of 5 Myr determined in our earlier investigation (Preibisch & Zinnecker 1999) based on a smaller sample of stars. The number of low-mass ($M_\star \sim [0.1 \ldots 0.5]\, M_\odot$) members is at least as high as expected from the know number of high-mass ($M_\star \gtrsim 3\, M_\odot$) association members and recent determinations of the field star IMF. Thus, there is no deficit of low-mass stars in Upper Scorpius.

1. Introduction

1.1. Motivation

It is important to study the population of low-mass ($M_\star \leq 2\, M_\odot$) pre-main sequence (PMS) stars in OB associations in order to derive the Initial Mass Function (IMF) over the full mass range, to understand their star formation history, and to compare these associations with low-mass star forming regions like T associations. Such a study can give us important information on the nature of the star formation process.

For many years it was thought that star formation is a bimodal process, i.e. that high- and low-mass stars form by different processes (e.g. Larson 1986; Shu & Lizano 1988). This scenario would seem to predict distinct formation sites for high-mass stars (the OB associations) and low-mass stars (the T-associations). However, it has also been known for a long time that at least some T associations do contain high-mass stars (e.g. Walter & Boyd 1991) and also that OB associations do contain low-mass stars (e.g. Herbig 1962). Thus, the bimodal star formation concept cannot be strictly correct. Nevertheless, there have been many indications that high-mass star forming regions (most notably starburst regions; cf. Leitherer 1998) contain much smaller numbers of low-mass stars than expected from the field IMF (see discussion in Zinnecker et al. 1993).

Generally, the low-mass IMF of OB associations is still very poorly known, mainly because

[1]Visiting Astronomer, Anglo-Australian Observatory.

low-mass PMS stars in OB associations are very difficult to find: The only completely reliable sign for their PMS nature is the strength of the 6708 Å Lithium line, requiring intermediate resolution spectroscopy for accurate measurement. Thus, the observational effort to identify the widespread population of PMS stars among the many thousands of field stars in the large areas covered by nearby OB associations is huge and up to now prevented further investigations. With the advent of extremely powerful multiple-object spectrographs, such as 2dF at the Anglo-Australian Telescope (cf. Taylor et al. 1997), which allows to take spectra of 400 targets simultaneously, huge spectroscopic surveys now become feasible.

1.2. The Upper Scorpius OB association

One of the best targets for an investigation of the low-mass IMF is the Upper Scorpius OB association (cf. Blaauw 1991; de Geus et al. 1989; Preibisch & Zinnecker 1999; de Zeeuw et al. 1999). Upper Sco is part of the large Scorpius-Centaurus association, the OB association nearest to the Sun. Upper Sco is the youngest subgroup of Scorpius-Centaurus and is located at a distance of only $D = 145$ pc (de Zeeuw et al. 1999). In contrast to the nearby ρ Oph molecular cloud (cf. Wilking 1991), which is located in front of the south-eastern edge of Upper Sco (de Zeeuw et al. 1999) and is well known for its strong star formation activity, the star formation process in Upper Sco is finished and there are neither dense molecular clouds nor deeply embedded young stellar objects. The Upper Sco area is essentially free of dense gas and dust clouds, and the association members show only very moderate extinctions ($A_V \lesssim 2$ mag). The Upper Sco association was very well investigated by the astrometry satellite Hipparcos and the population of high- and intermediate-mass ($M_\star \geq 3\,M_\odot$) stars is completely known (de Zeeuw et al. 1999; de Bruijne 1999). The members cover an area of about 120 square-degrees.

Several recent searches for low-mass stars have been conducted in Upper Sco. The first study was performed by Walter et al. (1994), who observed the optical counterparts of X-ray sources detected with the EINSTEIN satellite in a ~ 7 square-degree area and could identify 28 low-mass PMS stars. In another study, M. Kunkel investigated the optical counterparts of more than 200 ROSAT All Sky Survey (RASS) X-ray sources in a ~ 60 square-degree area in Upper Scorpius and Upper Centaurus-Lupus. A list of all stars in his sample can be found in Köhler et al. (1999), further information in Brandner et al. 2000 and Kunkel et al. 2000. Among those objects in this sample that are located in Upper Sco, 32 can be classified as new PMS stars (cf. Preibisch & Zinnecker 1999). A number of further searches (e.g. Meyer et al. 1993; Sciortino et al. 1998; Martin et al. 1998) were restricted to small subregions of the association. A recent deep search for very-low mass PMS star and brown dwarf candidates in Upper Sco was presented by Ardila et al. (2000). Their photometric survey covered an area of 14 square-degrees and yielded some 100 candidate members. Ardila et al. (2000) performed low-resolution spectroscopy of some of their candidates and classified 20 stars with strong Hα emission as potential members. If future, higher resolution spectroscopic observations would confirm the PMS status of these candidates, Upper Sco might contain an excess of brown dwarfs over the number predicted by the field star IMF.

The study presented in this paper is the third major step in our long term project to determine the star formation history and the IMF of the Upper Sco association. Our first step (Preibisch et al. 1998; P98 hereafter) was a spectroscopic survey for PMS stars among RASS X-ray sources in a 160 square-degree area in Upper Sco. The aim of this survey was to obtain a spatially complete (but flux-limited) sample of PMS stars over the *full area* of the association. This survey revealed 39 new PMS stars. In the second step (Preibisch & Zinnecker 1999; PZ99 hereafter) we investigated the star formation history in Upper Sco based on a sample of 98 PMS stars compiled from the studies mentioned above. We performed a detailed analysis of the HR diagram, taking proper account of the uncertainties and the effects of unresolved binaries, and derive ages and masses for the PMS stars. We found that the low-mass PMS stars have a mean age of about 5 Myr and show no evidence for a large age dispersion. This age agrees very well with the age of 5 – 6 Myr previously found for the massive stars (de Zeeuw & Brand 1985; de Geus et al. 1989). We concluded that the star formation process in Upper Sco was probably triggered by the shock wave of a supernova explosion in the nearby Upper Centaurus-Lupus association (as originally suggested by de Geus 1992 for the population of high-mass stars). The PMS sample of PZ99 is statistically complete for stellar masses down to $\sim 0.8\,M_\odot$.

1.3. Aim of our study

The aim of the study presented here is to reveal the full population of low- and very-low mass $\sim [0.1 \ldots 0.7]\,M_\odot$ stars in a representative area of Upper Sco. In combination with earlier studies this should allow a direct determination of the full IMF of an OB association, covering the stellar mass range from $\sim 0.1\,M_\odot$ up to $\sim 20\,M_\odot$, for the first time. In order to reach this aim, we must consider three important aspects.

First, *the study should be unbiased.* Essentially all known PMS stars in Upper Sco have been detected as counterparts of X-ray sources. On the one hand, this is the reason why most of the faint M-type stars, which are faint in X-rays too, are still missing from the current sample of known PMS stars. On the other hand, the X-ray selection might introduce a serious bias into the PMS sample, because one cannot yet fully exclude the possible existence of an "X-ray quiet" population of PMS stars. If there were such a population, it would be systematically missing from any X-ray selected sample. Similar problems exist with other indicators of stellar youth, such as Hα emission or infrared excess. We will therefore not use any preselection of candidate members but observe all stars with magnitudes that are consistent with being potential members.

Second, the observations should allow a *reliable classification of the PMS nature* of the stars. Neither photometric observations alone nor PMS indicators such as Hα emission or infrared excess provide a reliable way to discern between PMS stars and older field stars. Currently, the only convincing sign for the PMS nature of a star is the strength of the 6708 Å Lithium line, requiring intermediate resolution spectroscopy ($\Delta\lambda < 2$ Å) for accurate measurement.

Third, the observations should yield a *statistically meaningful sample* of PMS stars that is large enough to derive the IMF. Since at least $\gtrsim 100$ objects are needed to keep the statistical errors below 10%, we have to observe hundreds of targets to find enough PMS objects.

Considering these aspects, the only way to reach our aim is to perform a large multi-object intermediate-resolution spectroscopy survey.

2. Target selection

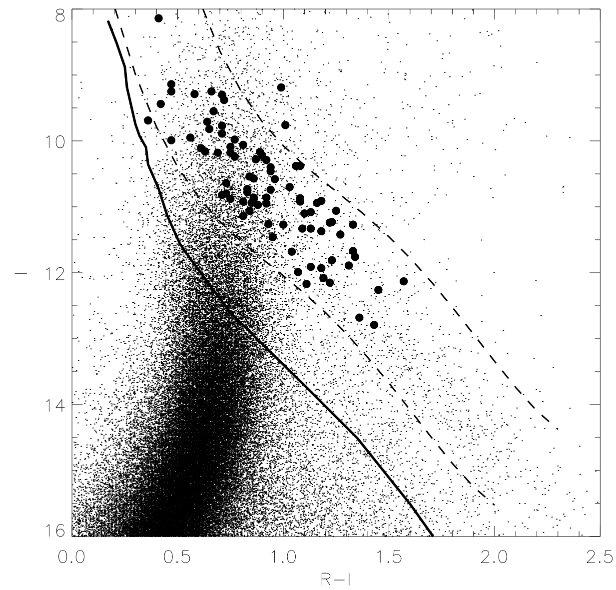

Fig. 1.— Color-Magnitude diagram for all stars (small dots) in the $6.5° \times 6.5°$ area of the UKST survey field 584 centered at $\alpha = 16^{\rm h}06^{\rm m}$, $\delta = -20°$ (B1950). The known PMS stars in Upper Sco from PZ99 are shown by the thick solid dots. The solid line shows the main-sequence at the distance of Upper Sco, the two dashed lines delimit the region of photometric PMS candidates based on the theoretical 5 Myr isochrone.

We already know the population of early-type association members (B- to A-type stars) from Hipparcos, and the population of solar-type stars (G- and K-type stars) from our previous study (P98; PZ99). What we are looking for now is the population of low-mass stars, i.e. basically the M-type stars. In order to compile a catalog of targets for our survey, we need positions and magnitudes of all objects in the field. We obtained these data from UKST Schmidt plates of the observed region. The R and I plates for the UKST survey fields 584, 515, and 516 were measured for us with SuperCOSMOS, the Royal Observatory Edinburgh's high-precision microdensitometer (see Hambly et

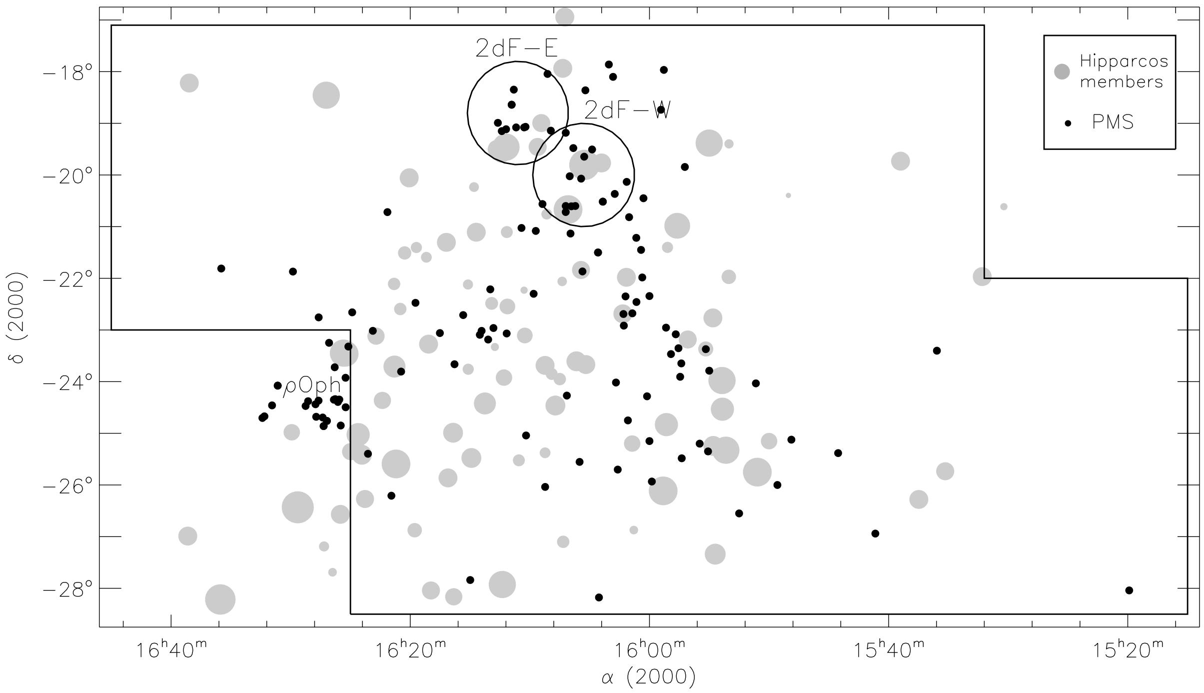

Fig. 2.— Map of the Upper Sco region. The area investigated by PZ99 is marked by the thick solid line. The small solid dots mark the positions of the low-mass PMS stars from PZ99. The Hipparcos high-mass members are shown as big grey dots, with symbol size proportional to the logarithm of their luminosity. The two circles show the positions of the two fields we have observed with 2dF, the eastern field 2dF-E and the western field 2dF-W.

al. 1998). After scanning, the data were processed to detect astronomical objects, and for all these objects their positions, celestial coordinates, instrumental magnitudes and other parameters were determined. The transformation of the instrumental magnitudes to standard photometric magnitudes was done as described in PZ99.

In Fig. 1 we show the color-magnitude diagram for UKST survey field 584, covering a 42 square degree area in Upper Sco. The already known PMS stars in Upper Sco populate a well defined locus in the diagram, with only very few outliers. This reflects the rather narrow distribution of ages found for the association members. The two dashed lines mark the band of expected locations for $\sim$ 5 Myr old PMS stars in Upper Sco. The stars between these lines are primary candidates for PMS stars. **However, we will not restrict our search for further PMS stars to the objects in this band.** As already noted above, it is our aim to perform an unbiased search. If we would observe only the stars within the band, i.e. around the “desired” isochrone, any investigation of the age distribution in the resulting sample would be meaningless because it would just reflect our selection criteria. We will therefore use very generous magnitude and color limits to define our target sample.

We want to find any potential late-type members, irrespective of their age and reddening. At the distance of Upper Sco, a 5 Myr old $1\,M_\odot$ star should have a magnitude of $I \sim 11.5$ (based on the predictions of the D’Antona & Mazzitelli (1994) PMS models). We used this magnitude as the bright limit for our target list. The faint limit was chosen so that we can obtain intermediate-resolution spectra with S/N of $\sim$ 100 in about 4 hours observing time. This corresponds roughly to $I \sim 15.5$. Any main sequence star at the distance of Upper Sco with $M \gtrsim 0.25\,M_\odot$ should be above this limit, so we are sensitive to all these stars irrespective of their age. Among the very-low-mass stars ($M \lesssim 0.2\,M_\odot$) this limit does not include main-sequence objects. However, even $0.1\,M_\odot$ objects with ages up to $\sim 20-30$ Myr are expected to be brighter than our faint limit. Since the association members are definitely not expected to be older than ~ 30 Myr, our survey will therefore still allow us to get a complete sample of all low-mass members of Upper Sco, to determine the age distribution, and the IMF of the association.

Since we are looking for late type stars, we also select the target stars according to their color, as e.g. an M0 star has an intrinsic color of $R-I \sim 0.9$. For this survey, we consider any star with $R-I \gtrsim 0.8$ as a target. In this way, all M-type and late K-type stars are included, while the bulk of the background field stars are avoided. This additional criterion does therefore not introduce any bias.

Our target selection criteria result in typically some 350 – 500 targets per 2° diameter field. We have selected several fields in the large area investigated in our previous studies (P98; PZ99) for observation with 2dF. The location of the observed fields can be seen in Fig. 2.

3. Observations and data analysis

The data were obtained in the nights of 8 and 9 June 2000 with the instrument 2dF[2] at the Anglo-Australian 3.9 m Telescope (AAT). The 2dF system is a fibre-feed multi-object spectrograph at the prime focus of the AAT that allows one to take spectra of 400 objects in a two degree diameter field.

3.1. Observing strategy

Our spectra cover the central part of the R-band. The magnitude range of our targets, $R \approx [12\ldots17]$, implies that the fluxes in the spectra of individual objects can vary by as much as a factor ~ 100. Since the 200 spectra on each detector are positioned only about 5 pixels apart, this can cause serious scattering problems if the spectrum of a faint object happens to lie next to the spectrum of a bright object on the CCD. It is therefore desirable to keep the magnitude difference in the target sample as small as possible. We therefore splitted our samples in one "bright" sub-sample and one "faint" sub-sample. The "bright" sub-sample contained all stars with $R \approx [12\ldots15]$, while the "faint" sub-sample contained the targets with $R \approx [14\ldots17]$. Stars in the $R \approx [14\ldots15]$ range are included in the "bright" as well as in the "faint" sub-sample. In this way we avoided the danger that some of the fainter targets in the "bright" sub-sample might yield only spectra with insufficient S/N, which would introduce a "gap" in our data. An additional advantage is that those stars for which two spectra are obtained can be used to check the internal consistency of our line-width and spectral type measurements.

The 2dF configuration program allows one to assign different priorities to the individual targets. Targets with high priority are then more likely to be observed than those with lower priority. Since the most promising candidates for new PMS stars are those located within the PMS "band" in the CMD (see Fig. 1), we assigned a higher priority to them as compared to the rest of the targets. It should be noted that the number of these "primary candidates" was about 100 per field. This means that most ($\sim \frac{3}{4}$) of the observed targets were **not** primary candidates. Our priority assignments therefore do **not** introduce selection effects in our data.

3.2. Field configuration

The initial step was to prepare a file containing accurate coordinates of all targets. This is already a critical task, because the fibre diameters of $2''$ require positions accurate to better than $0.5''$ to avoid significant light loss. Fortunately, the SuperCOSMOS data provide accurate enough coordinates for this purpose. The 2dF configuration program was then used to perform the allocation of objects to fibres in a 2dF field. This is a non-trivial task because one has to take into account several restrictions. For example, individual fibres cannot be placed too close to one another, and crossings of fibres must be minimized. Since any target sample will show a more or less pronounced inhomogeneity in the spatial distribution of the targets, e.g. by having small "clusters"of targets in a subarea of the field, it is often the case that not all targets can be reached by fibres. Therefore, the configuration program uses an iterative procedure to determine the most efficient allocation of

[2] A full description of 2dF can be found at `http://www.aao.gov.au/2df/index.html`

fibres to the individual targets. The algorithm can handle objects of different priorities by trying to allocate the highest priority objects first. In order to allow accurate sky subtraction, at least 20 fibres were not assigned to targets but put on empty sky positions.

Once the final allocation scheme was determined, the positioning of the individual fibres on the plate was done automatically by the 2dF positioner. A robotic gripper head moves over the field plate and places magnetic buttons attached to the fibre ends at the required positions on the plate. A prism at the head of each of the 400 fibres reflects the light from the object into the fibre. The two identical fibre spectrographs each receive 200 fibres. The detectors are 1024×1024 thinned Tektronix CCDs.

3.3. Observations

We used 1200 line/mm gratings in both spectrographs. The resulting spectra have a resolution of 1.8 Å ($R = 4000$) and cover the wavelength range from ~ 6150 Å to ~ 7250 Å.

Originally, we had intended to observe 4 individual 2dF fields. However, the weather conditions during our nights allowed us to observe only 2 fields, which we denote as 2dF-W and 2dF-E (cf. Fig. 2). For field 2dF-W we obtained a series of 4 individual 10 min exposures for the bright targets and a series of 8 individual 30 min exposures for the faint targets. The weather conditions were quite good with $1.2''$ seeing at the beginning of the night. During the observations the cloud coverage increased and forced a break in the observations. In the second half of the night the situation improved strongly and we could again get about 2 hours of exposure time.

The second night was characterized by marginal observing conditions during the first few hours. We could only obtain a series of 6 individual 10 min exposures for the bright targets in field 2dF-E. Shortly after the start of the first exposure for the faint targets of field 2dF-E the cloud extinction became so strong that we had to abort the observations.

3.4. Data reduction

Data reduction was performed with the 2dF data reduction system version 1.5. The data reduction system performs bias correction, flat fielding, tram-line mapping to the fibre locations on the CCD, optimal fibre extraction, cosmic ray rejection, arc identification, wavelength calibration, fibre throughput calibration and sky subtraction. The spectra were left on the natural system of the telescope/detector combination following flat-fielding.

3.5. Target statistics

Field 2dF-W contains 495 targets, among them 106 primary candidates, and field 2dF-E contains 512 targets, among them 99 primary candidates. In total, we could obtain 629 usable spectra of 576 individual stars. Among these are 13 previously known PMS stars, which we observed with the aim of using them as spectral standards. In field 2dF-W, 96 of 106 primary candidates, i.e. 86.8% were observed. In field 2dF-E, where we only could obtain spectra for the brighter stars, 61 of the 99 primary candidates, i.e. 62%, were observed. Some typical examples of our spectra are shown in Fig. 3.

4. Data analysis

4.1. Measurements of line widths

We used the IRAF[3] task *SPLOT* to determine the equivalent width of the 6708 Å Li line in all spectra. In most of our spectra the Li line can be readily distinguished from the nearby 6705 Å and 6710 Å Fe lines. The equivalent width was measured in two ways, first by integrating over the line profile, and second by fitting a Gaussian to the line profile. The mean of both values was used as the final equivalent width. For nearly all spectra the two values agree to within better than $\sim 10\%$. Among those 9 stars for which we obtained two usable spectra, the measured line widths typically show a scatter of $\lesssim \pm 0.075$ Å. For these stars we used the mean of the two line width measurements. Uncertain line width measurements resulted for a few spectra with rather low S/N; these are marked with colons in Table 1.

In our spectra of relatively bright stars with very good S/N we can clearly detect the Li line

[3]IRAF is distributed by the National Optical Astronomy Observatories, which are operated by the Association of Universities for Research in Astronomy, Inc., under cooperative agreement with the National Science Foundation.

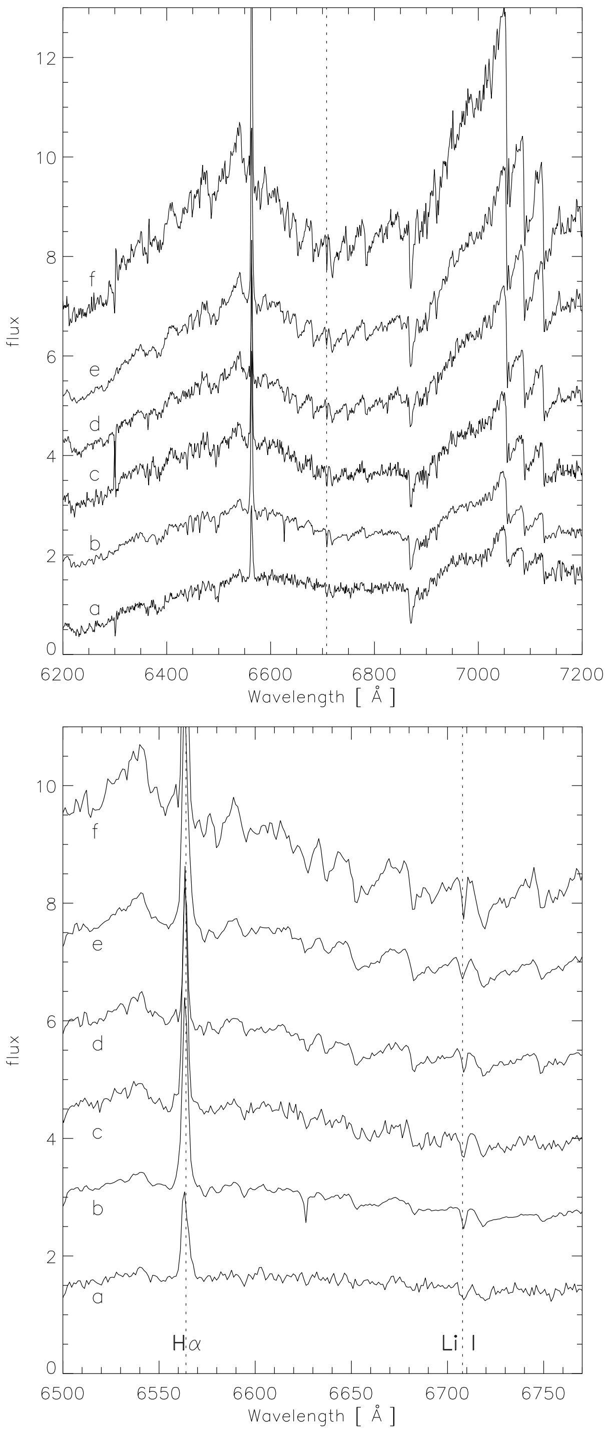

Fig. 3.— Typical examples of our 2dF spectra. Spectra of the following PMS stars are shown: a = 160954.4–190654 (M1), b = 160502.1–203507 (M2), c = 160823.5–191131 (M3), d = 160516.1–193830 (M4), e = 160350.4–194121 (M4.5), f = 160632.1–202053 (M5). The upper plot shows (nearly) the full wavelength range of our spectra, the lower plot shows details in the region of the Hα and Li I line.

with equivalent widths as low as $W \approx 0.04$ Å. For spectra with lower S/N the detection threshold is somewhat higher, around 0.1 Å. In order to get a homogeneous data set we will therefore consider as "Li-rich stars" all objects for which we find a Li line with $W \gtrsim 0.1$ Å. Among the 563 previously unobserved stars for which we could obtain spectra, 98 can be classified as Li-rich.

4.2. Determination of spectral types

For all Li-rich stars we determined the spectral type. In order to allow a reliable determination of the spectral types, we included those of the previously known Upper Sco PMS stars in our target samples that lie within our 2dF fields and are not too bright ($I > 11.5$). In total, there are 13 such stars from Walter et al. (1994; Sco29, 31, 32, 42a, 42b, 46, 51), Kunkel (RXJ 1607.0-1911), Martin et al. (1998; RXJ1612.1-1915, RXJ1614.4-1857, RXJ1613.7-1926, RXJ1613.1-1904), and Ardila et al. (2000; CTIO 56). The spectral types of these stars range from K5 to M5.

We used two different approaches for the determination of spectral types. First, we employed several different flux ratios over small wavelength ranges that are known to correlate with the spectral type. The ratios are defined as follows, where F denotes the flux integrated over the specified wavelength range in Å: $R4/R7 = F(6750-6844)/F(7000-7068)$ as defined by Prosser et al. (1991), $I1 = F(7020-7050)/F(6960-6990)$ and $I2 = F(6510-6540)/F(6370-6400)$ as defined by Martin & Kun (1996). These ratios showed a reasonably good linear correlation with the spectral types of our standard stars. Furthermore, we found that the flux ratios $T1 = F(7061-7088)/F(7024-7055)$ and $T2 = F(7095-7126)/F(7024-7055)$, which measure the relative strength of the TiO features near 7100 Å, also are well correlated to the spectral type. We computed these flux ratios for all standard spectra and determined the best linear fit between each flux ratio and the spectral type. Then we inverted these fits and determined the "best estimate" of the spectral type as the weighted mean of these relations, whereby the largest weight was given to the relation yielding the best correlation ($T1$, $T2$, $I1$) with the standard stars. Finally, we compared the best estimates for the spectral types determined from these ratio fits to the true spectral types of the standard stars. For the stars not later than M4 the rms deviation between estimated and true spectral types is 0.5 subtypes.

Additionally, we compared the overall appearance of the spectra against the grid of standards. In nearly all cases the spectral types estimated from this visual comparison agreed well (within 0.5 subtypes) with the types determined from the flux ratios. We assume our spectral types to be accurate to ± 0.5 subclass in most cases. Since the latest spectral type of our standards is M5, we cannot reliably classify those objects for which the flux ratios suggested spectral types later than M5; a visual inspection of these spectra, however, suggested that even the coolest objects in our sample are probably not much cooler than M5.

As expected, all of the Li-rich stars are found to be M-type or late K-type stars. Nearly all of these stars display the Hα line in emission. A plot of the Hα line-width versus spectral type is shown in Fig. 5.

4.3. Classification of PMS stars

We determined the pre-main sequence nature of a star by the strength of its 6708 Å Li I absorption line. Since Li is strongly diminished in very early phases of stellar evolution, a high Li content is a reliable indication for the youth of a star (e.g. Herbig 1962, D'Antona & Mazzitelli 1994). However, Li depletion is not only a function of stellar age, but also of stellar mass and presumably even depends on additional factors like stellar rotation (cf. Soderblom 1996). Not only PMS stars, but also somewhat older, though still relatively young zero-age main sequence stars, e.g. the G and K type stars in the $\sim 10^8$ years old Pleiades (c.f. Soderblom et al. 1993a), can display Li absorption lines. In order to classify stars as PMS, we thus have to consider a spectral type dependent threshold for the Li line width. Here we use the threshold as described in Preibisch et al. (1998).

From Fig. 4 one can see that all Li-rich stars in our 2dF sample lie above the PMS-threshold in the Li line width versus spectral type diagram. While this is not very surprising, since the PMS-threshold is quite low at the late spectral types of our stars, it is interesting to note that 97% of our Li-rich stars display quite strong Li lines with

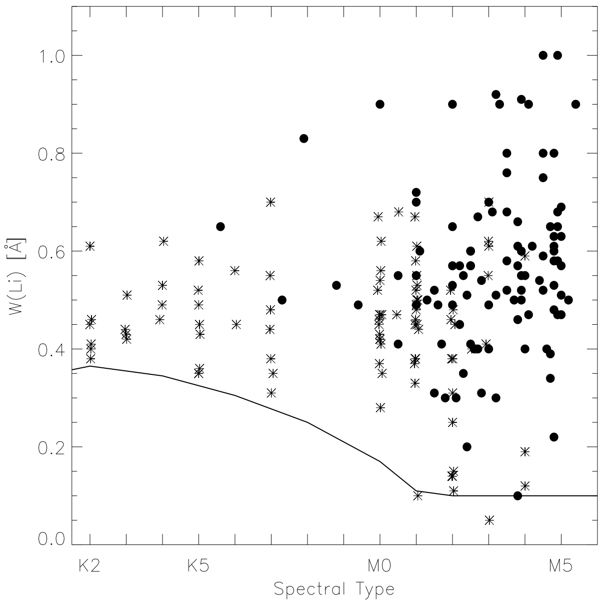

Fig. 4.— Equivalent width of the 6708 Å Li line versus the spectral type of the Li-rich stars found with 2dF (solid dots). The previously known PMS stars in Upper Sco (from PZ99) are shown as asterisks. The solid line shows the upper envelope for the Li line widths of stars in several young (≥ 30 Myr old) clusters and is used as a lower limit for the classification of PMS objects (see text for details).

$W > 0.3$ Å, and nearly 70% of our Li-rich stars display very strong Li lines with $W > 0.5$ Å. We conclude that all the Li-rich stars can be considered to be PMS stars. We believe that all these stars are T Tauri stars. However, since there is no generally accepted definition of T Tauri stars and some controversy about the naming conventions (e.g. Caillault et al. 1998; Martin 1998) we prefer the more cautious name PMS stars.

With only 3 exceptions, all our Li-rich stars show the Hα line in emission. This is another indicator for the youth of our objects, although by far not as convincing as the Li lines, because many main sequence M-stars also show Hα emission (e.g. Prosser et al. 1991). As the Hα emission line widths are below 10 Å for all but 10 objects, 90% of our PMS stars are weak-line T Tauri stars. The 10% fraction of classical T Tauri stars (CTTS) is quite similar to the fraction of $4/98 \sim 4\%$ in the PZ99 sample if we take into account that late M-

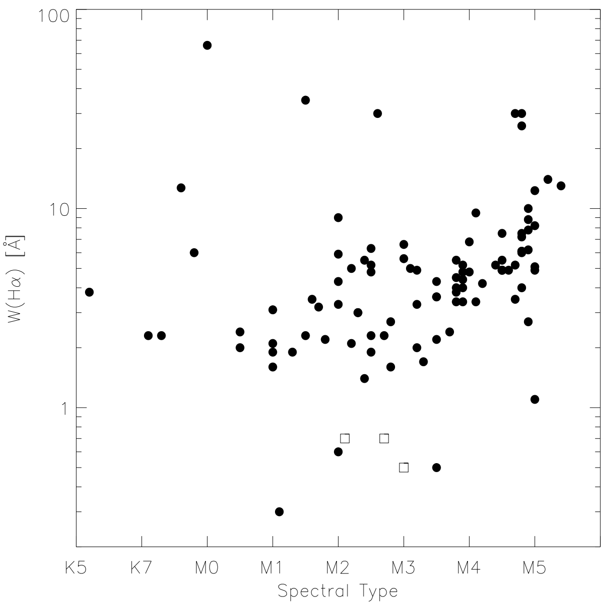

Fig. 5.— Equivalent width of the 6564 Å Hα line versus the spectral type for the Li-rich stars found with 2dF. Stars with Hα emission are shown as solid dots, those with Hα absorption as open squares.

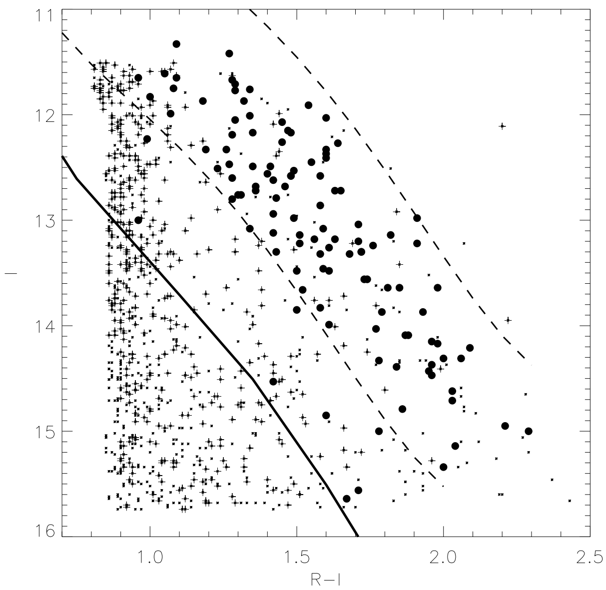

Fig. 6.— Color-Magnitude diagram for the targets of our survey. All objects in our target lists are shown as small dots. Stars that were observed with 2dF are shown as small crosses, and the Li-rich stars found with 2dF are shown as solid dots. The thick line shows the main sequence from Leggett (1992), the two dashed lines show the extension of the band defined by the previously known PMS stars in Upper Sco (cf. Fig. 1).

type stars generally display a higher ratio of Hα- to continuum-flux in their spectra than hotter stars. Our sample of new PMS stars again confirms that the fraction of CTTS in Upper Sco is much lower than typically found for regions with ongoing star formation, as has been already found by Walter et al. (1994), Martin et al. (1998), and PZ99. As discussed in PZ99, the low fraction of CTTS seems to be the consequence of the relatively large age of the stars as compared to the circumstellar disk survival time scale of a few Myr (see discussion in Bouvier et al. 1997) as well as the result of the presence of massive stars in Upper Sco that emit strong stellar winds, ionizing radiation and drive supernova shock-waves, which have accelerated disk dissipation.

4.4. Color-Magnitude Diagram

In Fig. 6 we show the color-magnitude diagram of our targets. One can see that all but 8 of the Li-rich stars lie within the band for primary photometric PMS candidates. In other words, only 8 of the 406 *non-primary candidate targets*, i.e. 1.7%, are Li-rich stars, whereas the corresponding fraction of Li-rich stars among the primary photometric PMS candidates is 77% (see below).

One can also see that nearly all objects which were classified as PMS stars spectroscopically by the strength of their Li absorption lines clearly lie well above the main sequence, confirming their PMS status.

4.5. Spatial distribution of PMS stars

Our 2dF survey revealed 98 new PMS stars in an area in which only 20 PMS stars were previously known (PZ99). This means that our survey increased the known number of PMS stars in this area by a factor of 5.

As we could not observe the faint targets in field 2dF-E, our sample of PMS stars is complete only for field 2dF-W. The term "complete" refers of course to the magnitude range of our target list; our survey is sensitive down to stellar masses

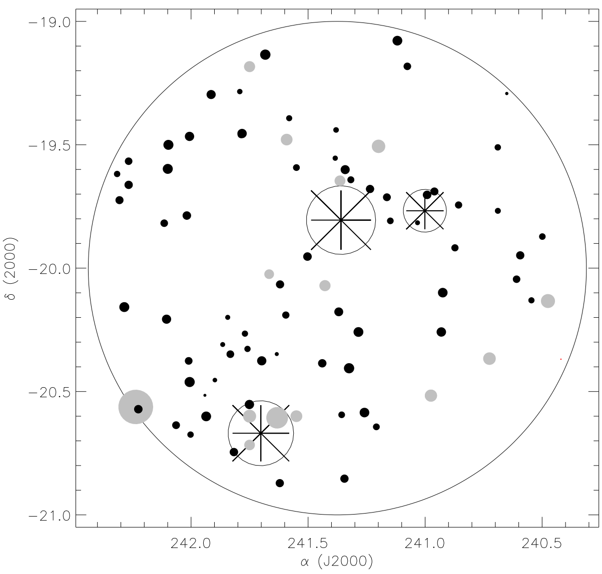

Fig. 7.— Map of field 2dF-W. Hipparcos members are shown by encircled asterisks, previously known PMS stars (cf. PZ99) as grey dots, and the new PMS stars detected in this study as black dots. The size of the individual symbols is proportional to the magnitude of the stars.

of $\sim 0.1\,M_\odot$ but probably not for sub-stellar objects (see below). Figure 7 shows the spatial distribution of the new PMS stars with respect to the previously known low-mass PMS stars (PZ99) and the Hipparcos high-mass members (de Zeeuw et al. 1999).

5. Masses and ages of the PMS stars

In PZ99 we determined ages and masses of the PMS stars in Upper Sco by placing them into the HR diagram and comparing their locations with the D'Antona & Mazzitelli (1994) PMS models. The much larger sample of low-mass PMS stars now known from our 2dF survey allows us to extend these investigations and to strengthen their statistical significance. We note that the last few years brought a considerable progress in the field of theoretical PMS models. For example, it is now possible to use observational constraints, such as dynamical masses in multiple systems, to check the validity of different models (cf. Luhman 1999; White et al. 1999). Our large sample of low-mass PMS stars is worth a careful analysis that should take into account this progress on the theoretical side. A detailed investigation of the HRD of Upper Sco will therefore be the topic of a forthcoming paper (Preibisch et al. in preparation). Here, we just want to perform a "quick-look" analysis of the new HRD for Upper Sco in order to compare it to the HRD presented in PZ99. For doing this, we used the same procedure as in PZ99 to determine the extinctions, luminosities, and temperatures of the stars and also compare the observational HRD to the PMS models of D'Antona & Mazzitelli (1994). Our new HRD is shown in Fig. 8.

5.1. Stellar ages and the star formation history

A detailed discussion of the HR diagram of the previously known PMS stars in Upper Sco has been presented in Preibisch & Zinnecker (1999). In that paper we derived constraints on the age distribution of the PMS stars and found that the low-mass PMS stars have a mean age of about 5 Myr and show no evidence for a large age dispersion. Since this age agrees very well with that derived for the massive stars (de Geus et al. 1989) and corresponds just to the time at which the shock wave from a supernova explosion in the nearby Upper Centaurus-Lupus association passed through Upper Sco (cf. de Geus 1992), we concluded that this supernova shock wave probably triggered a "mini-starburst" in Upper Sco.

In PZ99 we determined the mean age of the association members by modeling their distribution in the HRD. Our modeling procedure takes proper account of the observational uncertainties and the effects of unresolved binaries; it predicts a band of expected locations for the PMS stars given a specific mean age and age spread. This strategy has the advantage that one can derive constraints on the age distribution without the need to consider completeness corrections or to correct for the fact that the sample is composed of several subsamples covering different areas.

In Fig. 8 we have included the theoretical band of expected locations for the age distribution suggested by PZ99, i.e. a mean age of 5 Myr and no age spread. The theoretical expectation that 90% of the stars should lie within this band if the assumed age is correct, is very well confirmed by our data: 90 of the 98 new PMS stars are located within the band. This strongly supports our con-

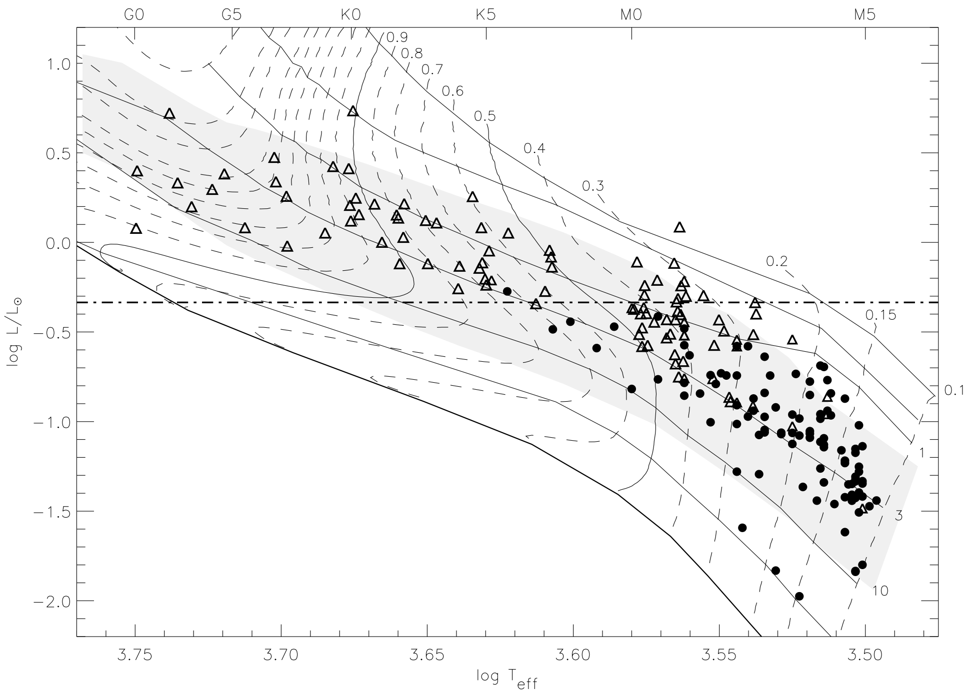

Fig. 8.— HR diagram for the PMS stars in Upper Sco. The previously known PMS stars from PZ99 are shown as triangles, the new PMS detected in this study are shown as solid dots. The dashed lines show the evolutionary tracks from DM94 and are labeled by their masses in solar units. The 1 $M_\odot$ and 0.5 $M_\odot$ track are shown as solid lines. The other solid lines show the DM94 isochrones for the ages of 0.1, 0.3, 1, 3, 10, and 30 Myr and finally the main sequence. The grey shaded band shows the region in which we expect 90% of the PMS stars to lie, based on the assumption of a common age of 5 Myr for all stars and taking proper account of the uncertainties and the effects of unresolved binaries (for details see text). The thick horizontal dashed-dotted line indicates the sensitivity limit of the X-ray observations that were of basis of the X-ray selected PMS sample (see PZ99).

clusions in PZ99 about the ages of the PMS stars in Upper Sco, i.e. a mean age of 5 Myr.

5.2. Stellar masses and the IMF of Upper Sco

In this preliminary analysis of the HRD we will restrict our investigation of the mass function to the comparison of the number of low-mass PMS stars to that of the high-mass members of Upper Sco. Since in field 2dF-E only the relatively bright targets could be observed, we can only consider the low-mass PMS stars in our field 2dF-W for this analysis.

5.2.1. Number of low-mass PMS stars

Since we could not observe all target stars, there are probably still some undetected PMS stars. As mentioned above, nearly all new PMS stars were found among the primary photometric candidates in the color-magnitude diagram. We therefore will assume that our observational completeness is identical to the fraction of the observed primary photometric candidates. Field 2dF-W contains 110 primary photometric candidates; among these were 4 previously known PMS stars that we included as spectral standard stars. We obtained spectra for 92 of the 106 new candidates and found 70 new PMS stars among them (7 new PMS stars were found among the targets that were not primary photometric candidates). Thus there are

$70 + 4 = 74$ PMS stars among the $92 + 4 = 96$ observed primary candidates, i.e. 77% of the primary candidates are PMS stars. 10 primary photometric candidates remained unobserved. If we assume that the fraction of PMS stars among these objects is the same as among the observed candidates, then we can expect 7.7 of these objects to be additional PMS stars. Thus the likely total number of PMS stars in our magnitude range in field 2dF-W is $70 + 4 + 7.7 + 7 = 88.7$.

For nearly all of our new PMS stars a comparison of their location in the HRD (Fig. 8) with the D'Antona & Mazzitelli (1994) models suggests masses between $0.1\,M_\odot$ and $0.5\,M_\odot$. We will therefore consider this mass range for our analysis of the IMF. In our field 2dF-W, 3 of the 81 known PMS stars, i.e. 4%, have a mass above $0.5\,M_\odot$ according to their position in the HRD. If we assume the same fraction among the 10 unobserved candidates, we find that the likely total number of PMS stars in the $[0.1 \ldots 0.5]\,M_\odot$ range should be $[81 - 3] + [10 \times (0.77 - 0.04)] \sim 85$. This number can now be compared with expectations from the field IMF based on the number of high-mass members of Upper Sco.

5.2.2. *Number of high-mass members*

The Upper Sco association was very well investigated by the astrometry satellite Hipparcos. De Zeeuw et al. (1999) investigated the kinematic membership of 1215 stars in Upper Sco and identified 120 association members. Brown (1998) investigated the mass function of these member stars. He found that the completeness limit of the Hipparcos sample corresponds to a mass of $\sim 2.8\,M_\odot$ and that 46 of the Hipparcos members have masses of $M_\star \geq 3\,M_\odot$. We can thus consider these 46 stars to be a complete sample of the high mass members in the mass range $[3 \ldots 20]\,M_\odot$. Due to the uncertainties in the membership determination (cf. de Bruijne 1999) and the mass determination this number is probably associated with an uncertainty of the order of $\pm 10\%$.

The spatial distribution of the Hipparcos stars can be seen in Fig. 9 in de Zeeuw et al. (1999). Nearly all objects are clustered in a $\sim 12^\circ$ diameter area. Therefore, the mean projected surface density of massive ($3\,M_\odot \leq M_\star \leq 20\,M_\odot$) association members in Upper Sco is about 0.41 per square-degree. For a 2° diameter field one thus can expect a mean number of 1.3 ± 0.1 massive stars. Our field 2dF-W contains 3 Hipparcos members, HIP 78702 (B9 V), HIP 78820 (B0.5 V), and HIP 78933 (B1 V). Since stars more massive than $3\,M_\odot$ should have spectral types of B8 or earlier (cf. Palla & Stahler 1993), there are two massive ($M_\star \geq 3\,M_\odot$) stars in our field, consistent with the expected number within the statistical uncertainties.

5.2.3. *Expected ratios based on the field IMF*

We can now compare the observed ratio of the number of low-mass ($0.1\,M_\odot \leq M_\star \leq 0.5\,M_\odot$) and high-mass ($M_\star \geq 3\,M_\odot$) stars with the corresponding figures predicted from different determinations of the field IMF. We will first consider the IMF as suggested by Scalo (1998), which can be described by a probability distribution with density

$$\frac{\mathrm{d}N}{\mathrm{d}M} \propto \begin{cases} M^{-1.2} & \text{for} \quad 0.1 \leq M/M_\odot < 1 \\ M^{-2.7} & \text{for} \quad 1 \leq M/M_\odot < 10 \\ M^{-2.3} & \text{for} \quad 10 \leq M/M_\odot < 100 \end{cases}$$

or, in shorter notation, $\alpha[0.1\text{–}1] = -1.2$, $\alpha[1\text{–}10] = -2.7$, $\alpha[10-100] = -2.3$. According to this IMF, the expected ratio is $\mathcal{R} := N(0.1 - 0.5\,M_\odot)/N(3 - 20\,M_\odot) = 25.3$.

A different IMF has been suggested by Kroupa (1995). It is given by $\alpha[0.08 - 0.5] = -1.3$, $\alpha[0.5 - 1] = -2.2$, $\alpha[1 - 100] = -2.7$. This IMF yields $\mathcal{R} = 43.6$.

Another representation of the IMF has been suggested by Kroupa (2000): $\alpha[0.02 - 0.08] = -0.3$, $\alpha[0.08 - 0.5] = -1.3$, $\alpha[0.5 - 100] = -2.3$, yielding $\mathcal{R} = 31.5$.

To summarize, these representations of the IMF suggest the ratio to be in the range $\mathcal{R} = [25.3 \ldots 43.6]$. Using this, the number of predicted low-mass stars in the $0.1 - 0.5\,M_\odot$ range should be $(1.3 \pm 0.1) \times \mathcal{R} = [30 \ldots 61]$.

5.2.4. *Observed distribution of masses*

The number of low-mass PMS stars as determined above for field 2df-W, 85, is clearly higher than the predictions based on the different field IMFs. However, before drawing any strong conclusions from this apparent excess of low-mass stars, one should consider the uncertainties associated with the number of low-mass members. A major source of uncertainty in the determination of stellar masses is the calibration of temperature as a function of spectral type (cf. Luhman 1999). While a detailed investigation of this issue will be postponed to another paper, we note that it might well be that the 2dF PMS stars cover a somewhat larger range of masses than predicted by the D'Antona & Mazzitelli (1994) tracks.

Another aspect we have to consider here is that our field 2dF-W covers only a relatively small fraction ($\sim 3\%$) of the full association. Since the spatial distribution of association members cannot be expected to be absolutely homogeneous, we have to consider the possibility of statistical fluctuations in the projected density of the members. To investigate this, we have studied the distribution of all primary photometric candidates in the full ~ 42 square-degree area of UKST survey field 584 that contains our 2dF fields. This ~ 42 square-degree area contains 993 primary photometric candidates. Thus, the mean number of primary photometric candidates per $2°$ diameter field is about 74, while our field 2dF-W actually contains 106 primary photometric candidates, 43% more than the mean. If we assume the fraction of PMS stars among the primary photometric candidates to be constant over the full field, the *mean* number of PMS stars in a randomly selected $2°$ diameter field should be therefore 58, rather than 85 as we find in field 2dF-W. This number is now quite consistent with the range of expectations from the different field IMF models.

In summary, our results suggest that the number of low-mass PMS stars is at least as high as expected from the field IMF, and there is *no deficit of low-mass stars*. The most simple way to characterize the mass function is assuming a power-law with constant slope over the full mass range. Our numbers from above yield $\alpha[0.1-20] \sim -2.1 \pm 0.1$ as a zeroth order approximation. This is somewhat higher, but quite similar to the Salpeter (1955) value of $\alpha = -2.35$ (which, however, was originally derived for the range of high- and intermediate mass stars only). The mean slope we find is also quite similar to the high-mass IMF determination of Brown (1998), who found $\alpha[3-20] \sim -1.9$.

6. Conclusions

Our 2dF survey reveals 98 new low-mass PMS stars in a ~ 6 square-degree area in Upper Sco. A (preliminary) analysis of their locations in the HR diagram suggests that the new low-mass stars show the same rather narrow age distribution around 5 Myr that we had previously derived for a smaller and less complete sample of Upper Sco members. This confirms our previous suggestion that the star formation process in Upper Sco can be characterized as a super-nova triggered mini-starburst. As far as the mass function of Upper Sco is concerned, we find that there are at least as many, perhaps even more, low-mass stars than expected from the known number of high-mass members and recent field IMF determinations. For the mean slope of the IMF of Upper Sco over the full mass range we find $\alpha[0.1-20] = -2.1 \pm 0.1$, which is quite similar to the slope of the high-mass IMF of Upper Sco and the Salpeter IMF.

We thank Terry Bridges for support during our 2dF observations. We also would like to thank the SuperCOSMOS Group at the Royal Observatory Edinburgh for scanning the UKST plates for us.

REFERENCES

D'Antona, F., Mazzitelli, I., 1994, A&AS 90, 467

Ardila D., Martin E., Basri G., 2000, AJ 120,479

Blaauw A., 1991, In: Lada C.J., Kylafis N.D. (eds.) The Physics of Star Formation and Early Stellar Evolution, NATO ASI Vol. 342, p. 125

Bouvier J., Forestini M., Allain S., 1997, A&A 326,1023

Brandner W., Zinnecker H., Alcala J.M., et al., 2000, AJ 120,950

Brown A.G.A., 1998, In: The Stellar Initial Mass Function, eds. G. Gilmore, D. Howell, ASP Conf Ser. Vol. 142, p. 45

de Bruijne J.H.J., 1999, MNRAS 310,585

Caillault J.-P., Briceno C., Martin E.L., Palla F., Wichmann R., 1998, in: *10th Cambridge Workshop on Cool Stars, Stellar System, and the Sun*, eds. B. Donahue & J. Bookbinder, ASP Conference Series Vol. 154, p. 237

de Geus E.J., 1992, A&A 262,258

de Geus, E.J., de Zeeuw, P.T. & Lub, J., 1989, A&A 216, 44

Hambly N.C., Miller L., MacGillivray H.T., Herd J.T., Cormack W.A., 1998, MNRAS 298,897

Herbig G.H., 1962, Adv. Astron. Astrophys., 1,47

Köhler R., Kunkel M., Leinert C. Zinnecker H., 1999, A&A 365,541

Kroupa P., 1995, ApJ 453, 358

Kroupa P., 2000, Astronomische Gesellschaft Meeting Abstracts, Vol. 16, p. 10

Kunkel M., Brandner W., Yorke H.W., et al., 2000, ApJS, submitted

Larson R.B., 1986, MNRAS 218,409

Legett S.K., 1992, ApJS 82,351

Leitherer C., 1998, In: The Stellar Initial Mass Function, eds. G. Gilmore, D. Howell, ASP Conf Ser. Vol. 142, p. 45

Luhman K.L., 1999, ApJ 525,466

Martin E.L., 1998, AJ 115,351

Martin E.L., Kun M., 1996, A&AS 116,467

Martin E.L., Montmerle T., Gregorio-Hetem J., Casanova S., 1998, MNRAS 300,733

Meyer M.R., Wilking B.A., Zinnecker H., 1993, AJ 105,619

Palla F., Stahler S.W., 1993, ApJ 418,414

Preibisch Th., Zinnecker H., 1999, AJ 117,2381 (PZ99)

Preibisch Th., Guenther E., Zinnecker H., Sterzik M., Frink S., Röser S., 1998, A&A 333,619 (P98)

Prosser C., Stauffer J., Kraft R.P., 1991, AJ 101,1361

Salpeter E.E., 1955, ApJ 121,161

Scalo J.M., 1998, In: Gilmore G., Howel D. (eds.) The stellar intial mass function, ASP Conference Series Vol. 142, p. 201

Sciortino S., Damiani F., Favata F., Micela G., 1998, A&A 332,825

Shu F.H., Lizano S., 1988, In: Stellar Matter, Moran J.M., Ho P.T.P. (eds.), Gordon & Breach, p. 65

Soderblom D.R., 1996, In: Pallavicini R., Dupree A.K. (eds.) 9th Cambridge Workshop on Cool Stars, Stellar System, and the Sun, ASP Conference Series Vol. 109, p. 315

Soderblom D.R., Jones B.F., Balachandrian S., et al., 1993, AJ 106,1059

Taylor K., Cannon, R, Watson F.G., 1997, Proc. SPIE Vol. 2871, p. 145

Walter, F.M. & Boyd, W.T., 1991, ApJ 370, 318

Walter, F.M., Vrba, F.J., Mathieu, R.D., Brown, A., & Myers, P.C., 1994, AJ 107,692

White R.J., Ghez A.M., Reid I.N., Schultz G., 1999, ApJ 520,811

Wilking B.A., 1991, In: Reipurth B. (ed.) Low Mass Star Formation in Southern Molecular Clouds, ESO Scientific Report No. 11, p. 159

de Zeeuw P.T., Brand J., 1985, In: van den Woerden H., Boland W. (eds.) Birth and Evolution of Massive Stars and Stellar Groups, Reidel, Dordrecht, p. 95

de Zeeuw P.T., Hoogerwerf R., de Bruijne J.H.J., Brown A.G.A., Blaauw A., 1999, AJ 117,354

Zinnecker H., McCaughrean M.J., Wilking B.A., 1993, In: Levy E.H., Lumine J.I. (eds.) Protostars and Planets III, University of Arizona Press, p. 429

This 2-column preprint was prepared with the AAS LaTeX macros v5.0.

Table 1: Li rich stars in Upper Sco detected in our 2dF survey.

star [J2000]	W(Li)	W(Hα)	SpT	star [J2000]	W(Li)	W(Hα)	SpT
[hhmmss.s–ddmmss]	[Å]	[Å]		[hhmmss.s–ddmmss]	[Å]	[Å]	
2dF160159.7–195219	0.47	–2.7	M 5	2dF160716.0–204443	0.68	–3.6	M 4
2dF160210.9–200749	0.65	–3.5	M 5	2dF160719.7–202055	0.57	–2.3	M 3
2dF160222.4–195653	0.4 :	–6.6	M 3	2dF160722.4–201158	0.5 :	–14.0	M 5
2dF160226.2–200241	0.47	–4.9	M 5	2dF160727.5–201834	0.9 :	–13.0	M 5
2dF160236.2–191732	0.4 :	0.7	M 3	2dF160735.5–202713	0.75	–4.9	M 5
2dF160245.4–194604	0.3 :	0.7	M 2	2dF160739.4–191747	0.52	–2.3	M 2
2dF160245.4–193037	0.51	–1.1	M 5	2dF160744.5–203602	0.50	–4.8	M 4
2dF160325.6–194438	0.20	–1.4	M 2	2dF160745.8–203055	0.3 :	–2.0	M 3
2dF160329.4–195503	0.40	–4.9	M 5	2dF160800.5–204028	0.34	–5.2	M 5
2dF160341.8–200557	0.3 :	–2.2	M 2	2dF160801.4–202741	0.83	–2.3	K 8
2dF160343.3–201531	0.49	–3.5	M 2	2dF160801.5–192757	0.52	–3.6	M 4
2dF160350.4–194121	0.59	–4.9	M 5	2dF160802.4–202233	0.6 :	–6.1	M 5
2dF160357.9–194210	0.35	–3.0	M 2	2dF160804.3–194712	0.91	–5.2	M 4
2dF160407.7–194857	0.22	–4.0	M 5	2dF160815.3–203811	0.57	–1.9	M 3
2dF160418.2–191055	0.76	–0.5	M 4	2dF160823.2–193001	0.49	–6.0	K 9
2dF160428.0–190434	0.55	–3.4	M 4	2dF160823.5–191131	0.92	–4.9	M 3
2dF160428.4–190441	0.68	–5.0	M 3	2dF160823.8–193551	0.72	–2.1	M 1
2dF160435.6–194830	0.63	–7.2	M 5	2dF160825.1–201224	0.41	–2.0	M 1
2dF160439.1–194245	0.61	–3.8	M 4	2dF160827.5–194904	0.57	–12.3	M 5
2dF160449.9–203835	0.65	–7.8	M 5	2dF160843.1–190051	0.8 :	–7.5	M 5
2dF160456.4–194045	0.54	–5.2	M 4	2dF160845.6–182443	0.7 :	0.5 :	M 3
2dF160502.1–203507	0.57	–5.9	M 2	2dF160900.7–190852	0.53	–12.7	K 9
2dF160508.3–201531	0.58	–4.3	M 4	2dF160903.9–193944	0.31	–2.7	M 3
2dF160508.4–201532	0.46	–5.5	M 4	2dF160904.0–193359	0.80	–2.2	M 4
2dF160516.1–193830	0.50	–2.4	M 4	2dF160908.4–200928	0.66	–4.0	M 4
2dF160517.9–202420	0.41	–5.2	M 3	2dF160913.4–194328	0.54	–1.6	M 3
2dF160521.9–193602	0.50	–1.9	M 1	2dF160915.8–193706	0.90	–1.7	M 3
2dF160522.7–205111	0.1 :	–4.5	M 4	2dF160916.8–183522	0.55	–3.0	M 2
2dF160525.5–203539	0.48	–6.1	M 5	2dF160933.8–190456	0.49	–3.3	M 2
2dF160528.5–201037	0.55	–1.9	M 1	2dF160936.5–184800	1.0 :	–10 :	M 5
2dF160531.3–192623	0.58	–8.8	M 5	2dF160943.8–182302	0.9 :	–9.5	M 4
2dF160532.1–193315	0.61	–26.0	M 5	2dF160946.4–193735	0.49	–1.6	M 1
2dF160545.4–202308	0.31	–35.0	M 2	2dF160954.4–190654	0.70	–3.1	M 1
2dF160600.6–195711	0.8 :	–7.5	M 5	2dF160959.4–180009	1.0 :	–4.9	M 5
2dF160611.9–193532	0.63	–8.2	M 5	2dF161010.4–194539	0.49	–5.6	M 3
2dF160619.3–192332	0.52	–5.5	M 5	2dF161014.7–191909	0.45	–2.1	M 2
2dF160622.8–201124	0.53	–6.0	M 5	2dF161024.7–191407	0.51	–3.3	M 3
2dF160628.7–200357	0.58	–30.0	M 5	2dF161031.9–191305	0.50	–2.3	K 7
2dF160629.0–205216	0.68	–6.2	M 5	2dF161039.5–191652	0.53	–4.3	M 2
2dF160632.1–202053	0.69	–5.1	M 5	2dF161043.9–192225	0.67	–2.3	M 3
2dF160643.8–190805	0.65	–3.8	K 6	2dF161115.3–175721	0.55	–2.4	M 1
2dF160647.5–202232	0.41	–3.2	M 2	2dF161116.6–193910	0.47	–3.4	M 4
2dF160700.1–203309	0.65	–0.6	M 2	2dF161118.1–175728	0.55	–4.8	M 4
2dF160702.1–201938	0.39	-30.0	M 5	2dF161123.0–190522	0.40	–6.8	M 4
2dF160704.7–201555	0.61	–4.2	M 4	2dF161133.6–191400	0.6 :	–4.8	M 3
2dF160707.7–192715	0.57	–5.0	M 2	2dF161156.2–194323	0.60	–6.3	M 3
2dF160708.7–192733	0.52	–4.0	M 4	2dF161420.2–190648	0.9 :	–66 :	M 0 :
2dF160710.0–191703	0.9 :	–9.0	M 2 :	2dF161433.6–190013	0.4 :	–30 :	M 3
2dF160854.0–203417	0.57	–3.4	M 4	2dF161120.4–191937	0.51	–5.5	M 2

Notes: The source name in the first column consists of the J2000 coordinates of the stars. Star 2dF161420.2–190648 displays a strongly veiled spectrum; this object might be identical to RXJ 1614.3–1906b from Martin et al. (1998).